Polymer Chain Phase Transition Analysis Through Molecular Dynamics Simulations

Matthew Rao

1. Introduction

Polymers have seen widespread usage in spacecraft for a multitude of reasons, ranging from having optimal weight-to-strength ratios to protection against heat and radiation. Such polymers, however, can undergo phase transitions when exposed to extreme temperatures. The phases can be broadly classified into two distinct classes: folded, or globular states, as well as unfolded, or extended states. In space, the low temperatures can contribute to unwanted phase transitions for the polymers, causing folding or causing the material to become brittle. The challenge, therefore, lies in optimizing conditions to prevent polymer folding at these conditions, as well as understanding forces that contribute to particle interactions.

This project aims to increase understanding of phase transitions in polymers by calculating factors like harmonic and Lennard-Jones forces, radius of gyration, and end-to-end distances to provide a representative molecular dynamics simulation. In doing so, the results will provide insights into how chemical and temperature conditions can be optimized to ensure that the polymers are operating at maximum efficiency.

2. Methodologies

The molecular dynamics simulations were carried out in various conditions – although temperature was varied to understand temperature-driven phase transitions, the spring constant and repulsive Lennard-Jones potential were also varied to inform how the chemical properties of the polymer can contribute to efficiency.

Polymers can best be represented as molecules made up of repeating subunits. For the purposes of this report, the polymers will be modeled using the Bead-Spring model. This model represents the repeating subunit monomers as beads connected by harmonic springs.

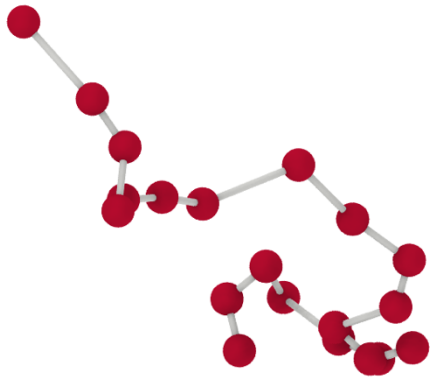

Figure 1. Bead-spring model of the polymer chain. Adapted from *Computational Problem Solving in the Chemical Sciences*, Lecture 25.

Since the polymer consists of multiple parts, it is therefore important to also take into account the multiple forces at play. Looking at Figure 1, the beads have Lennard-Jones forces interacting with each other, whereas the harmonic springs have a spring constant that contributes

to the overall energy of the system. Therefore, we can best categorize our interactions into bonded and non-bonded interactions, being harmonic potentials and Lennard-Jones potentials, respectively.

$$U_{\text{bond}}(r) = \frac{1}{2}k(r - r_0)^2 \textbf{ (1)}$$

$$U_{LJ,rep}(r) = \begin{cases} 4\epsilon_{rep}[(\sigma/r)^{12} - (\sigma/r)^6 + 1/4], & r < 2^{1/6} \\ 0, & r \geq 2^{1/6} \end{cases} \textbf{ (2)}$$

$$U_{\text{LJ,att}}(r) = 4\epsilon_{\text{att}}\left[\left(\frac{\sigma}{r}\right)^{12} - \left(\frac{\sigma}{r}\right)^{6}\right] \textbf{ (3)}$$

$$U_{\text{total}} = \sum_{\text{bonds}} U_{\text{bond}}(r_{i,i+1}) + \sum_{\substack{i,j \\ |i-j|=2}} U_{\text{LJ,rep}}(r_{ij}) + \sum_{\substack{i,j \\ |i-j|>2}} U_{\text{LJ,att}}(r_{ij}) \textbf{ (4)}$$

In this case, Equation 1 represents the harmonic bond potential between adjacent beads, with *k* representing the spring constant, *r* representing the distance between adjacent beads, and r_0 representing the equilibrium bond length. For the potential between the beads, the Lennard-Jones potential was used. Beads separated by one spacer experienced repulsion (Eq. 2), whereas beads separated by more than one spacer experienced attractive potentials (Eq. 3). In both cases, ϵ_{rep} and ϵ_{att} model the repulsive and attractive potentials, respectively, and σ models the Lennard-Jones potential parameter. When calculating our total potential energy, the harmonic potential energy is simply summed up alongside the repulsive and attractive Lennard-Jones potentials (Eq. 4).

The simulation process can be broken down into smaller steps. The position and velocities of the polymer chain were first initialized in a box of size 100 units, with the polymer containing 20 subunits. The positions were randomly adjusted based on randomly generated unit vectors, whereas the velocities were randomly sampled from the Maxwell-Boltzmann distribution. Then, over the course of 10,000 timesteps, the total forces of the polymer were computed and summed (Eq. 5-7).

$$F_{\text{bond}} = -\frac{dU_{\text{bond}}}{dr} = -k(r - r_0)\hat{r} \textbf{ (5)}$$

$$F_{\text{LJ,rep}}(r) = 24\epsilon_{\text{rep}}\left[\left(\frac{\sigma}{r}\right)^{12} - \frac{1}{2}\left(\frac{\sigma}{r}\right)^{6}\right]\frac{\hat{r}}{r} \textbf{ (6)}$$

$$F_{\text{LJ,rep}}(r) = 24\epsilon_{att}\left[\left(\frac{\sigma}{r}\right)^{12} - \frac{1}{2}\left(\frac{\sigma}{r}\right)^{6}\right]\frac{\hat{r}}{r} \textbf{ (7)}$$

The positions and velocities of the polymer subunits were subsequently updated using Verlet Integration (Eq. 8-9), and then the thermostat was applied. Every 100 timesteps, a rescaling factor was applied to the velocities to ensure that they fit the Maxwell-Boltzmann distribution, in which case the instantaneous temperature was first computed (Eq. 10), and then the updated velocity was calculated (Eq. 11).

$$v\left(t + \frac{\Delta t}{2}\right) = v(t) + \frac{\Delta t}{2m}F(t) \textbf{ (8)}$$

$$r(t + \Delta t) = r(t) + v\left(t + \frac{\Delta t}{2}\right)\Delta t \textbf{ (9)}$$

$$T_{\text{inst}} = \frac{2KE}{3NK_B} \textbf{ (10)}$$

$$v_f = v_i\sqrt{\frac{T_{\text{target}}}{T_{\text{inst}}}} \textbf{ (11)}$$

We observe that KE represents kinetic energy, N represents the number of particles, and K_B represents the Boltzmann constant. Throughout the simulation, the periodic boundary conditions were applied by computing the modulus between position and box size.

After running the given steps in the simulation, the properties of the polymer were then computed. The radius of gyration (Eq. 12) and end-to-end distance (Eq. 13) of the polymer were calculated. Subsequently, the harmonic potential energy was computed alongside the attractive and repulsive components of the Lennard-Jones potential and summed up (Eq. 1-4).

$$R_g = \sqrt{\frac{1}{N}\sum_{i=1}^{N}|r_i - r_{\text{cm}}|^2} \textbf{ (12)}$$

$$r_{\text{cm}} = \frac{1}{N}\sum_{i=1}^{N} r_i \textbf{ (13)}$$

The coordinates of the polymer subunits were taken and subsequently plotted in 3D space. Additionally, radius of gyration, end-to-end distance, and potential energy were all plotted against temperature. The simulation was run for 3 independent variables. For the first experiment, the temperature was varied from 0.1 to 1.0 to observe the effects of folding at lower temperatures. The second experiment involved maintaining the temperature at 0.1 and varying the spring constant from 0.1 to 3.0. Finally, the last experiment involved maintaining the temperature at 0.1 and varying the repulsive epsilon component from 0.1 to 3.0. Temperature was kept at low values to find optimal values for the other variables to prevent folding in extreme conditions.

3. Results

3.1 Effect of temperature variation

Within the first experiment, temperature was varied while the other variables were held constant. The spring constant was kept at a value of 1.0, whereas the ϵ_{rep} value was also kept at 1.0 reduced units. Since extreme temperatures cause polymer subunit interactions to occur, the temperature was varied over the course of 10 values, ranging from 0.1 to 1.0. In this case, three metrics were used: radius of gyration, end-to-end distance, and potential energy. The radius of gyration was plotted to provide understanding about phase transitions. Since it measures the distribution of mass for rotation, a lower value corresponds to more folding. The end-to-end distance provides a measure of the distance from the first subunit to the last subunit. Similarly, a low end-to-end distance is indicative of higher folding. Finally, potential energy helps us determine the interactions present. Higher potential energy means that more energy is stored, and in tandem, these metrics provide a baseline for observing the results and understanding how and

when phase transitions occur. For the temperature experiment, Figure 2 shows increasing radius of gyration as temperature increases. While there were certainly fluctuations in this value from start to finish, the overall trend shows a positive relationship between the two variables. Furthermore, it was observed that the end-to-end distance also increased when the temperature was increased (Fig. 2). Though this value began to level out near the end, the beginning to end trend again shows a positive relationship. Finally, looking at potential energy, a relatively steady and positive relationship was also observed as potential energy increased as temperature was increased (Fig. 2). As temperature was increased, a phase transition seemed to have occurred, with both the radius of gyration and the end-to-end distance increasing. This indicates a further distance of mass away from the center and a further distance of end particles away from each other. Additionally, there was a jump in the temperature at around T = 0.45. This drastic change in potential energy is indicative of a phase change.

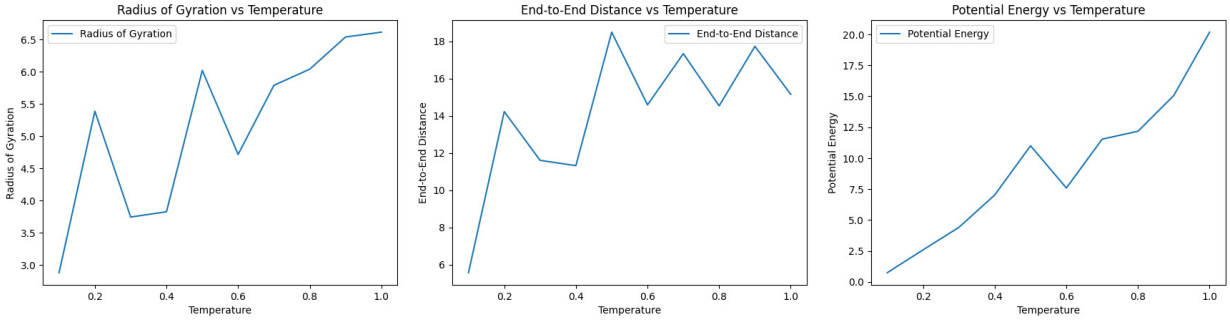

Figure 2. Metrics of radius of gyration, end-to-end distance, and potential energy of the polymer as a function of temperature

The polymer structures at various temperatures also provide insights into what a phase transition might look like. At a low temperature of T = 0.1, the polymer appears to be very compact, being heavily folded in on itself (Fig. 3). As temperature was increased, the polymer appeared to have a phase transition, being more elongated at T = 0.50. Finally, at the highest temperature, the particle appeared to fold a bit, with the ends being closer together, though without the compactness observed at T = 0.10.

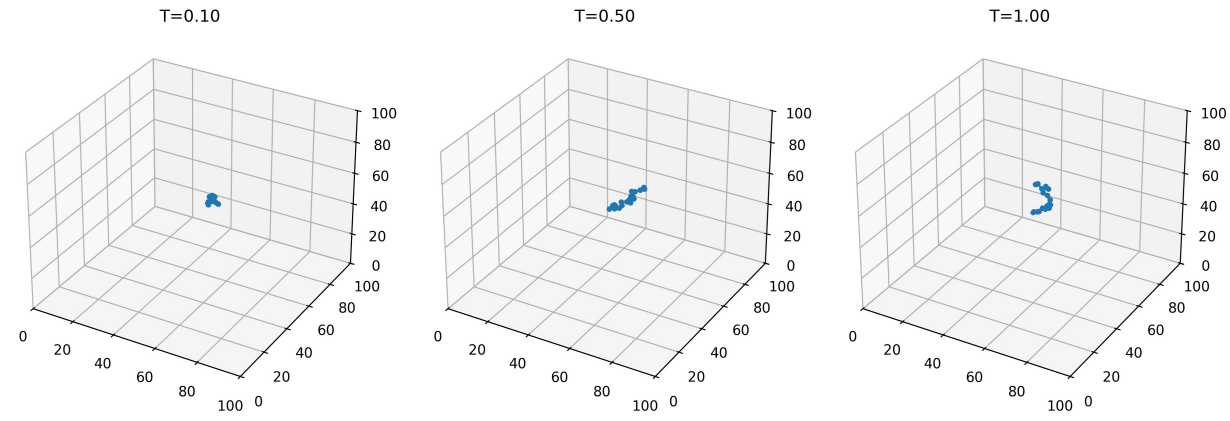

Figure 3. Structures of polymer at values of T=0.10, 0.50 and 1.00.

3.2 Effect of spring constant variation

For the spring constant simulation, the spring constant was varied from 0.1 to 3.0 over the course of 30 values. This ensured that a wide range of values was captured to identify optimal spring constant values at low temperatures. Temperature was maintained at 0.1 for this simulation, and all other values were held constant. Examining the effects of the spring constant, the radius of gyration decreased overall as the spring constant was increased. Significant fluctuations were observed; however, the overall radius was smaller after a larger spring constant was applied (Fig. 4). Looking at the end-to-end distance, large fluctuations can also be observed. However, it can also be seen that the end-to-end distance decreases slightly from the beginning to end, if only slightly (Fig. 4). Potential energy was observed to increase as the spring constant increased, though again, lots of fluctuations were observed. The results show a phase transition in terms of greater folding as the spring constant was increased, as both the radius of gyration and end-to-end distance decreased.

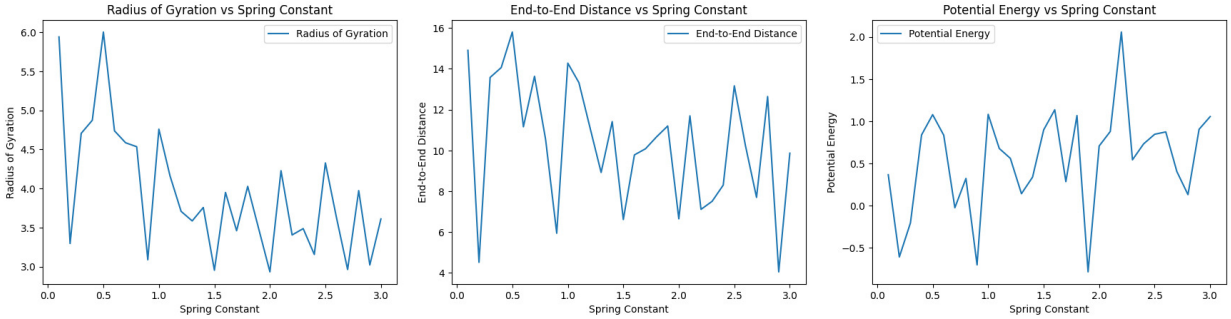

Figure 4. Metrics of radius of gyration, end-to-end distance, and potential energy of the polymer as a function of the spring constant

Examining the polymer configurations at low temperatures, the polymer appeared to be unfolded, or in an extended state at a spring constant of 0.10 (Fig. 5). As this, value was increased, however, the polymer appeared to become more compact, especially at a value of 2.00. At a k-value of 3.00, there was less folding, though the end-to-end distance showed that the polymer was not as extended as it was at a low spring constant.

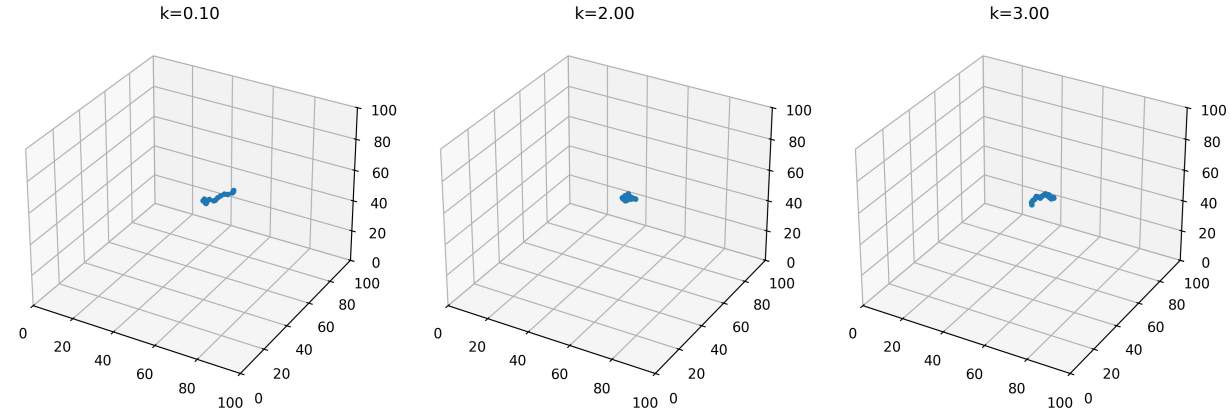

Figure 5. Structures of polymer at values of k=0.10, 2.00 and 3.00

3.3 Effect of repulsive epsilon variation

Like the spring constant, ϵ_{rep} was also varied from 0.10 to 3.00 across 30 values, with temperature being kept at a low value of 0.10 reduced units. As the reduced epsilon value was increased across trials, the radius of gyration experienced many fluctuations (Fig. 6). No clear trend could be observed from the graph. Likewise, the end-to-end distance appeared to experience many fluctuations as the repulsive epsilon value was increase (Fig. 6). The potential energy value was also shown to not have an observable trend, with fluctuations but no clear increase or decrease from beginning to end. Thus, unlike its predecessors, varying the ϵ_{rep} seemed to produce no observable phase transitions.

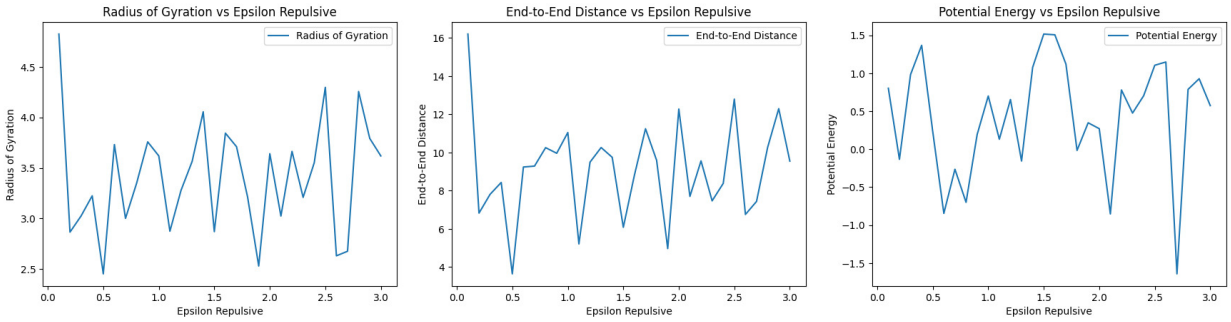

Figure 6. Metrics of radius of gyration, end-to-end distance, and potential energy of the polymer as a function of ϵ_{rep}

Examining the polymer configuration, the polymer appeared to be relatively compact at all epsilon repulsive values (Fig. 7). At a low value of 0.10, the polymer appeared to be very folded and compact. Similarly, at a higher value of 2.00, there was what appeared to be less, but still observable folding. At a value of 3.00, the polymer was still observed to have folded and globular characteristics.

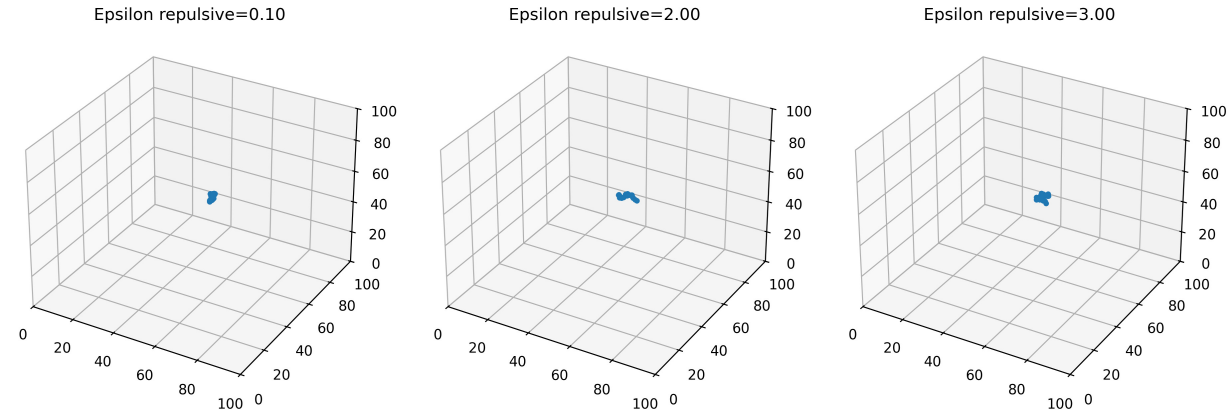

Figure 7. Structures of polymer at values of ϵ_{rep} = 0.10, 2.00 and 3.00

4. Discussion

4.1 Effect of temperature on polymer phase transitions

Temperature was observed to have effects on the globular and extended states of the polymer. As shown in Figure 2, an increase in temperature was associated with a higher radius of

gyration and a higher end-to-end distance. Thus, from its folded globular state, the mass was distributed further away from the center, and the distance from the initial to end subunit also generally increased. A limitation of the end-to-end distance, however, can be observed in Figure 3, in which the polymer appears to adopt a somewhat extended state, though the initial and end particles are curved toward each other, thus lowering the overall end-to-end distance. The results align with what we expect: since extreme temperatures appear to have effects on polymer folding, at a low temperature we would expect a globular state. At higher temperatures, the polymer would be expected to unfold. Furthermore, the increasing potential energy indicates that as the polymer unfolds, the attractive Lennard-Jones potential energy becomes less negative. That is, more potential energy is stored. This aligns with our expectations.

We can estimate a phase change to have occurred from about T=0.45 to T=0.6. In this region, all three metrics have distinctive jumps, with the potential energy jump being the most notable. For the rest of the potential energy data, the trend appears to be relatively smooth. Therefore, we can say that the best evidence for a phase transition occurs in this temperature region.

For the polymers in our simulation, it is therefore ideal to have higher temperature conditions to prevent folding. However, in external scenarios where temperature is difficult to control, having other variables of interest can make polymer folding more preventable. Since all three variables increased with temperature, there is evidence to suggest that a phase transition did occur.

4.2 Effect of spring constant on polymer phase transitions

Varying the spring constant seemed to have less pronounced effects on the phase transitions of the polymer. Though the radius of gyration did decrease as a whole, there were large fluctuations in the data, with the noise making interpretation difficult. End-to-end distance had less pronounced effects than the radius of gyration – again, there was an overall decrease in this value, but this data also had a lot of variability. Finally, potential energy of the system actually increased, though again, there was a lot of variability present (Fig. 4). A higher spring constant indicates more "rigidness" in terms of the bonds. Therefore, at higher values of k, there is less flexibility for the bonds. Due to the high fluctuations throughout the entire MD simulation, it cannot be said for certain that a phase transition actually occurred.

Overall, since radius of gyration and the end-to-end distance decreased with the increasing spring constant, it can be said that the optimal value for the spring constant should be low. Since the spring constant was initialized at a low value and the smallest amount of folding was present at these conditions, a lower spring constant is optimal. Furthermore, at k=0.10, the polymer's extended state (Fig. 5) is pronounced. At higher values of 2.00 and 3.00, respectively, this state is not present, though it cannot be said that a fully globular state is observed either. At a value of 2.00 for k, the polymer appeared to be very compact, whereas at a value of 3.00, the polymer appears somewhat extended, though the ends of the polymer curve toward each other. A definitive phase transition cannot be said to have occurred due to the large variability in the data. While potential explanations from the fluctuations can be attributed to conformational fluctuations or limited sampling, this makes phase transitions harder to define. However, it can be said that a lower value of k appears to be optimal for lower temperatures.

4.3 Effect of ϵ_{rep} on polymer phase transitions

Surprisingly, varying ϵ_{rep} had limited, if not negligible effects on the phase transitions of the polymer. Again, there were lots of fluctuations present in the graphs of all 3 metrics, along with no distinguishable phase transitions from the data. There was no clear difference in change from beginning to end, and while the data fluctuated, the average appeared to remain constant throughout all 3 graphs (Fig. 6). At higher values for ϵ_{rep}, it was expected that more repulsions between adjacent subunits would decrease folding as the repulsive forces would dominate. This was not the case that we observed. Throughout all values of epsilon repulsive at lower temperatures, the polymer appeared to remain folded (Fig. 7).

There could be a variety of reasons for why ϵ_{rep} had negligible effects on the system and why no phase transitions occurred. The most likely factor is that this force is only present between adjacent subunits. Alternatively, ϵ_{att} is present between all non-adjacent subunits. Therefore, the attractive forces could be more significant than the repulsive forces at a lower temperature. To prevent folding at lower temperatures, ϵ_{rep} does not appear to be a relevant factor to adjust.

5. Conclusion

For temperature itself, the results align with what we would expect. Steady unfolding was observed in which temperature was increased, showing that lower temperatures are indeed related to globular states. In applying this to varying ϵ_{rep} and the spring constant, varying ϵ_{rep} was found to have no significant effects at lower, space-like temperatures. This was attributed to the fact that this potential is only present between adjacent subunits, whereas the attractive potential was present between all non-adjacent subunits. Therefore, attractive potentials would be more dominant. To maintain simplicity in future experiments, ϵ_{rep} = 1.00 can be kept.

For the spring constant, it was observed that less folding occurred at lower values for k. Therefore, we can say that in designing polymers, a lower spring constant is preferred, specifically k = 0.10. While future studies can examine the effects of longer polymers and how they react to various extreme conditions. Additionally, future studies could examine more factors, like ϵ_{att} and how that relates to polymer folding. Overall, polymers with weak bonds at low temperatures appear to offset the polymer folding, helping to maintain the extended state.